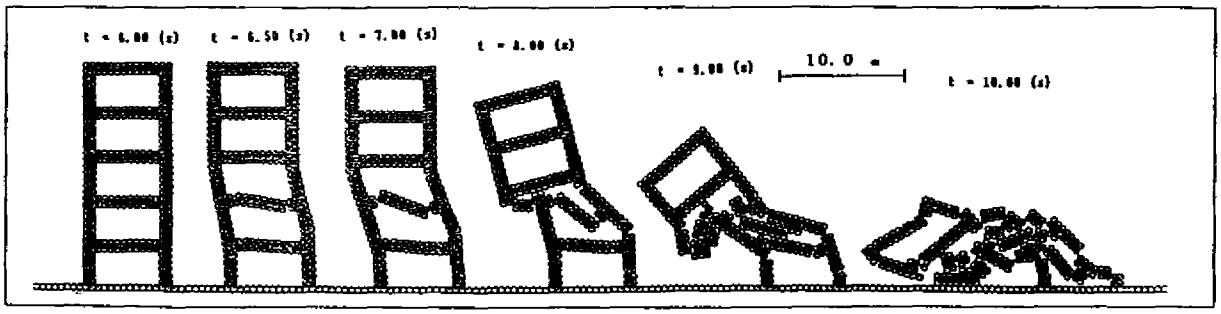


*Figure 4. Seismic response analysis of a slender building*
*(Case 2: Example of earthquake damage to weak-column-type buildings)*

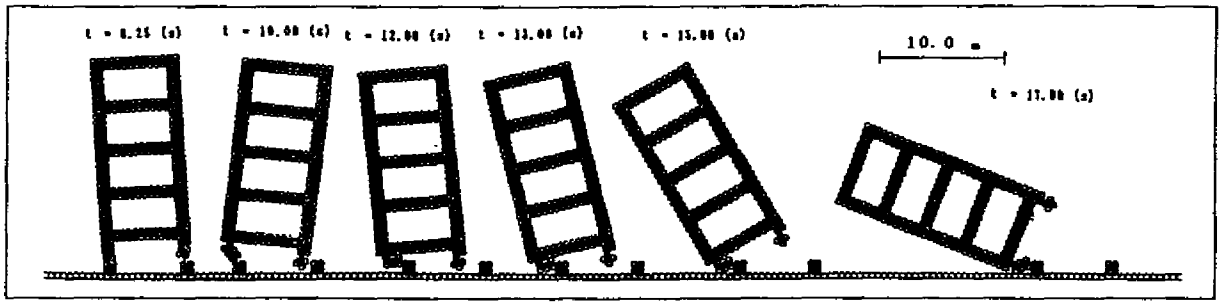


*Figure 5. Seismic response analysis of a slender building*
*(Case 3: Collapse of a slender building due to resonance)*

## 3. NUMERICAL RESULTS

To study the mechanism of collapse of structures due to past earthquakes, Meguro and Hakuno simulated various modes of collapsed structures, some of which are shown in Figures 6 to 8 (Hakuno and Meguro, 1993). After the 1995 Kobe earthquake, these types of structural collapse were observed in the affected areas (Photos 1-3).

In addition to the collapse of houses and building structures, elevated bridges of highways and railways were also severely damaged due to the 1995 Kobe earthquake. Since the earthquake occurred early in the morning, fortunately, casualties due to the damage of civil infrastructures such as highways and railways were not so many. If the earthquake had hit during daytime when the people were outside and using infrastructures, many people may have been killed or severely injured due to the collapse of these structures. Photos 4 and 5 show the collapse of elevated bridges of Hanshin Expressway. Considering the damage in Photo 4, although the piers didn't collapse but suffered some damage at the bottom, two adjacent simple-beam decks fell down due to dislocation of the bearing supports (Figure 9). Seventeen piers spanning over 630 m of pilz-type bridges were destroyed and the bridges collapsed (Photo 5). To study the collapse mechanism of these elevated bridges, the fracture process of the damage was simulated using the EDEM.

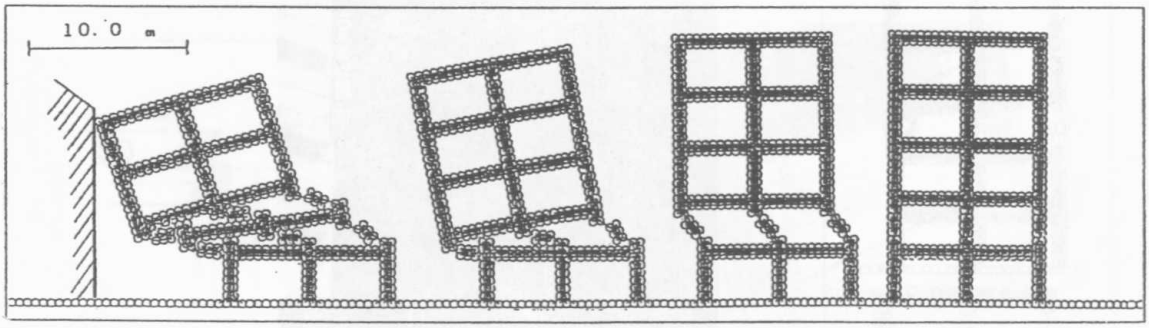


*Figure 6. EDE simulation of the tumbling-type collapse*

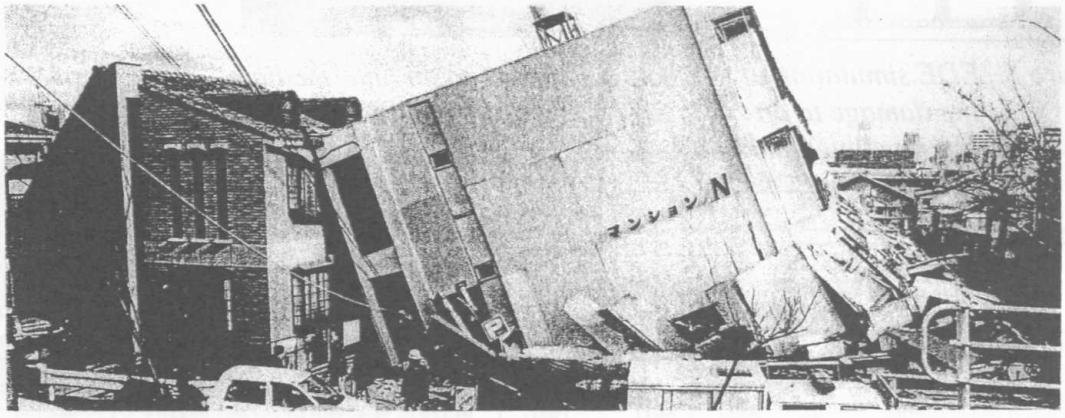


*Photo 1 Tumbling-type collapse of buildings*

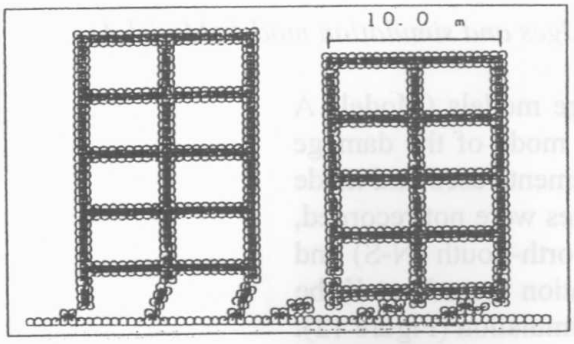


*Figure 7. EDE simulation of the damage to the first floor collapse-type*

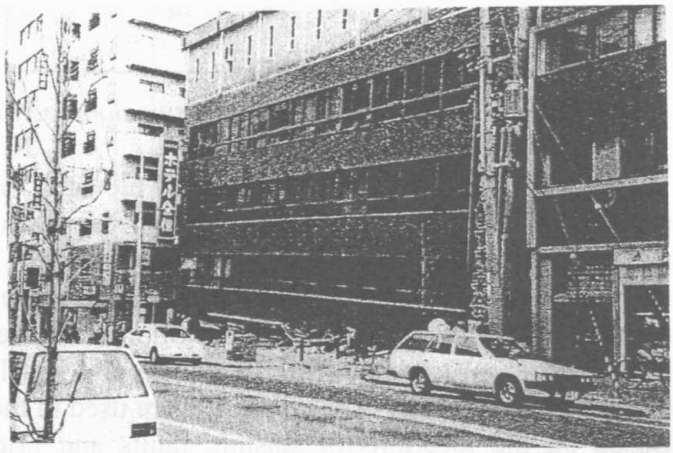

*Photo 2 Damage to the first floor collapse-type*

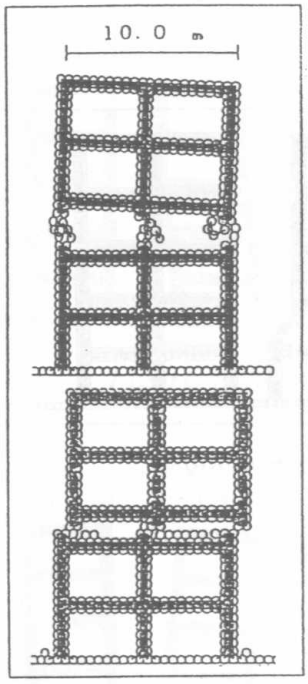


*Figure 8. EDE simulation of the damage to an intermediate floor collapse-type*


*Photo 3 Damage to an intermediate floor collapse-type*

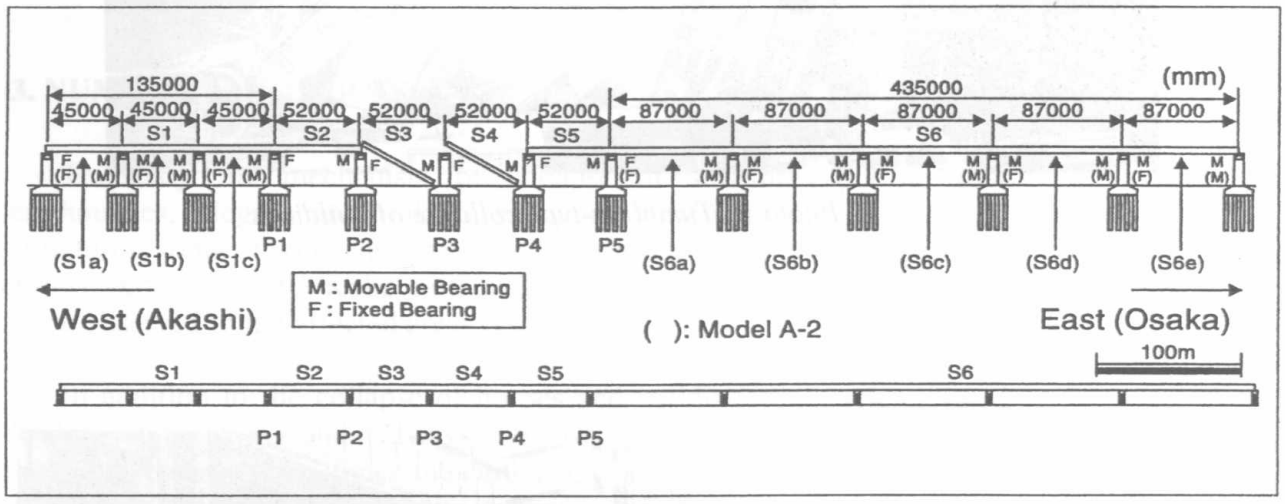


*Figure 9. Overview of the objective damaged bridges and simulation model (Model A)*

Figures 9 to 11 show the damaged elevated bridge models (Models A and B) for EDE simulation. Considering the fracture mode of the damage and computational time, we reduced the number of elements used and made the model simple. Since the ground motion at these sites were not recorded, numerical integrated displacement motion from the North-South (N-S) and East-West (E-W) components of the ground acceleration records at Kobe Marine Meteorological Observatory were used in the simulation (Figure 12). Based on the locations of seismic faults and bridges, and their collapse modes, E-W component was used for the Model A, and N-S component was used for the Model B.

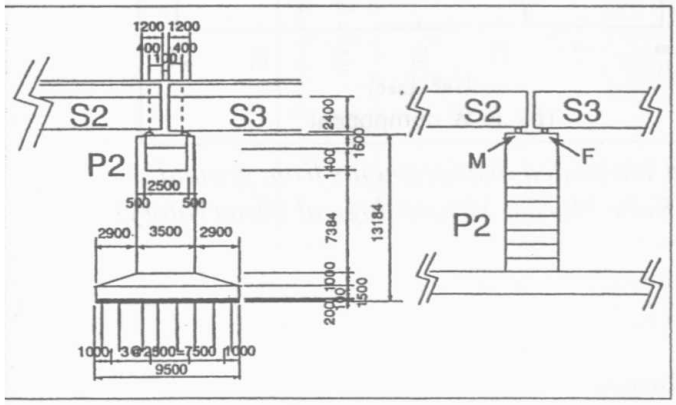


*Figure 10. Size of the bridges and close up of the simulation model (Model A)*

*Photo 4 Damage to elevated expressway bridges (Fallen two adjacent simple-beam decks)*

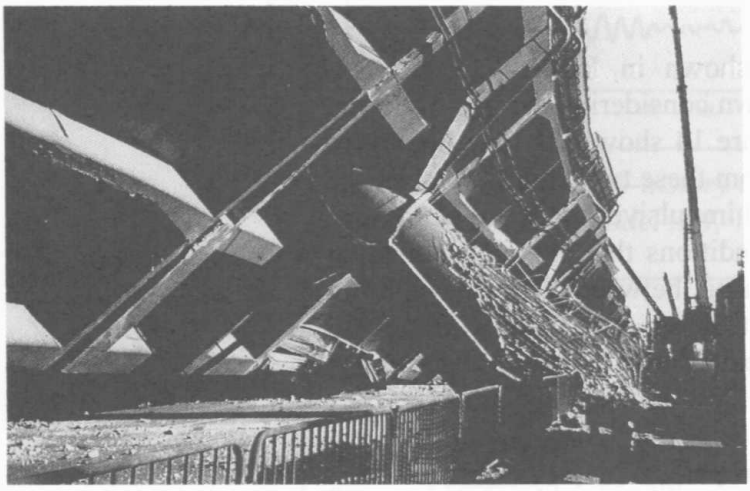

*Photo 5 Collapse of pilz-type bridges*

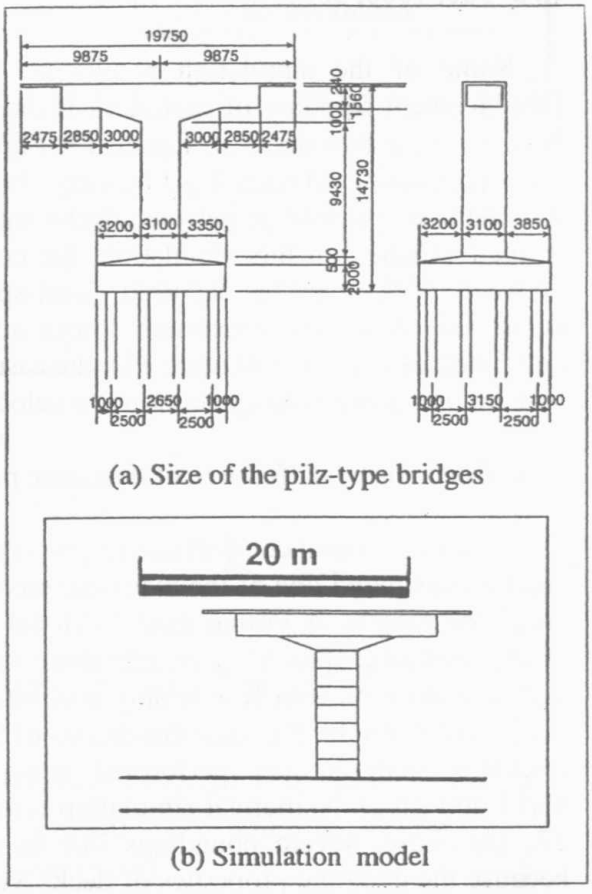


*Figure 11. Size of the pilz-type bridges and simulation model (Model B)*

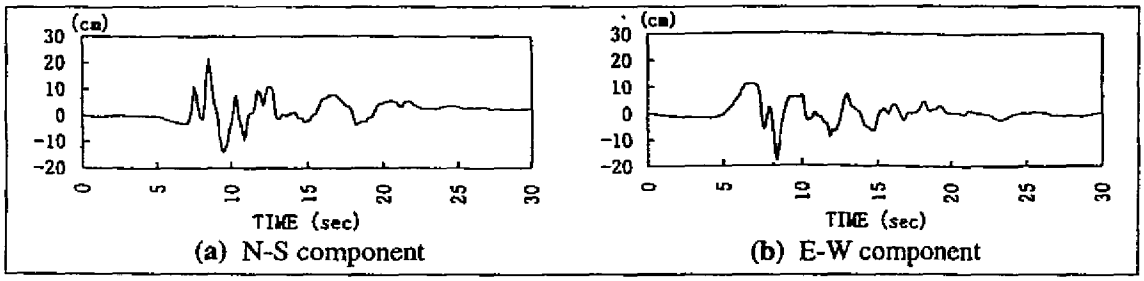


*Figure 12. Input ground motions (Numerical integrated displacements from ground acceleration records observed at Kobe Marine Meteorological Observatory)*

### 3.1 Simulation Results Using Model A

**Effects of the time lag of seismic load at the bases:**

Using the Model A in Figure 9, a series of simulations with and without consideration of time lag due to wave propagation were carried out. Namely, one case without input time lag, and four cases with the lag based on the assumption that the seismic wave in Figure 12 (b) propagated from the left (east) to the right (west) with different apparent wave velocity (Va=500, 1000, 3000, 5000, $\infty$ m/s).

Some of the simulation results are shown in Figures 13 and 14. Displacement response of each deck is drawn considering the gap of 10 cm between each two decks in Figure 13. Figure 14 shows the time history of the forces acting on each fixed bearing. From these two figures, we can see that there are poundings between decks and impulsive forces are acting due to their effects. In this simulation, the conditions that although pounding between decks can be occurred, joint-spring between elements are not destroyed. When the maximum forces acting on each fixed bearing are compared of five cases (Figure 15), the case of Va=3,000 m/s is the severest case among acceptable apparent wave velocities.

**Effects of the difference of dynamic properties between decks:**

As a big difference of dynamic properties among S1, S2 to S5, and S6 can be considered one of the main reasons of the collapse, next, we tried to study the effects. A virtual model (Model A-2) was made by dividing the continuous long-span S1 deck into three simply supported (S1a-S1c) decks and also S6 deck into five simply supported decks (S6a-S6e) as shown in the Figure 9. Under the same conditions of the previous simulation, dynamic response analysis was performed using the apparent wave velocity, Va=3,000 (m/s). Numerical simulation results are shown in Figures 16 and 17. This case, severe poundings like in the previous case are not seen because the dynamic properties of decks S1 and S6 became similar to those of S2 to S5 decks by dividing them. With the comparison of these two results, it can be noted that the effects of the difference of dynamic properties due to the different structural type had an important role in the mechanism of collapse.

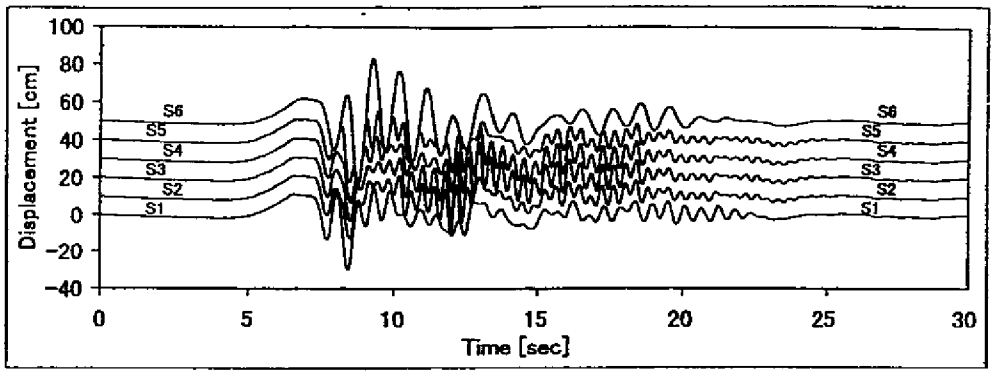


*Figure 13. Dynamic displacement response of each deck (Model A-1, Va=3,000 m/s)*

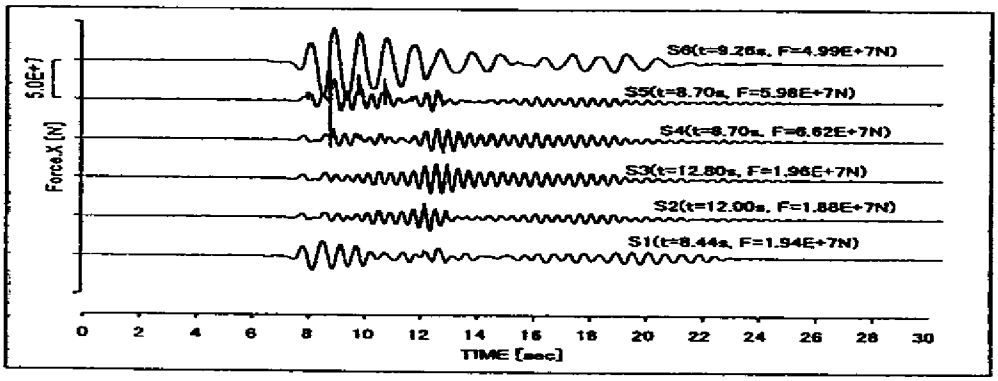


*Figure 14. Time-history of forces acting on fixed bearings (Model A-1, Va=3,000 m/s)*

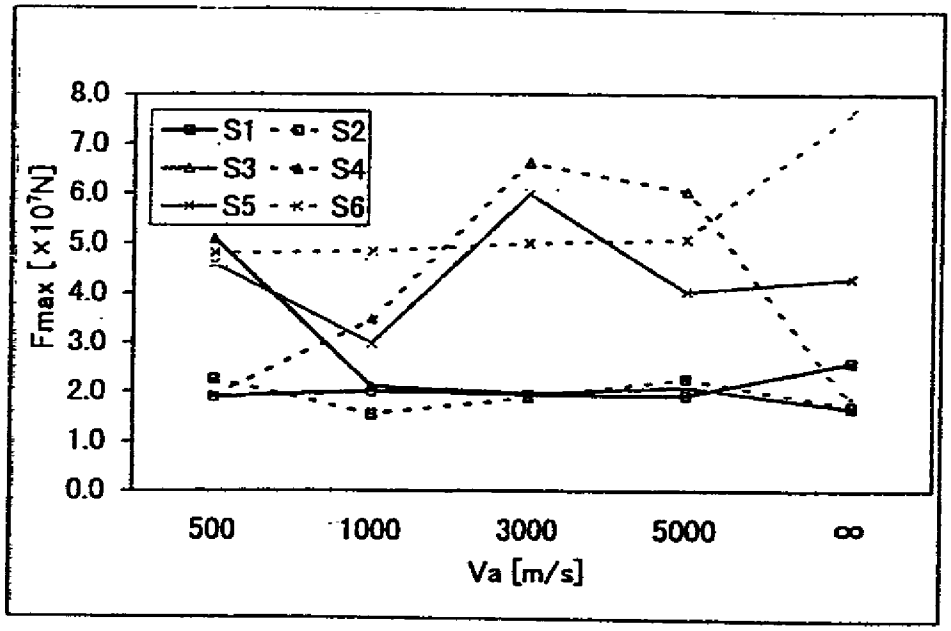


*Figure 15. Comparison of maximum force acting on fixed bearing (Model A-1)*

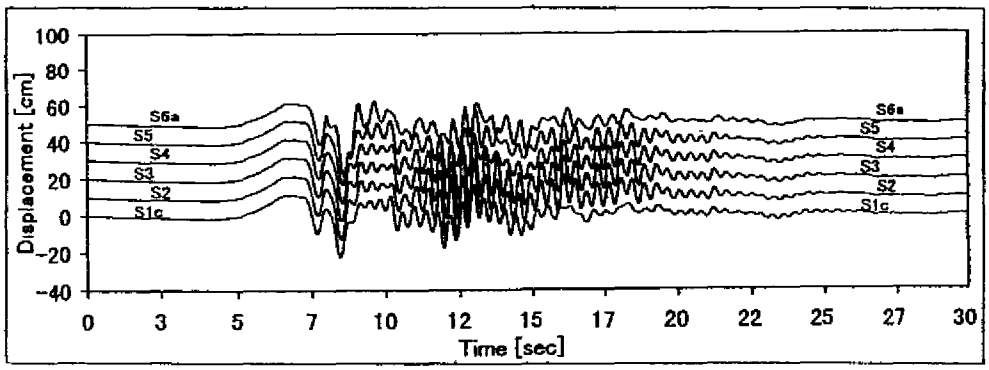


*Figure 16. Dynamic displacement response of each deck (Model A-2, Va=3,000 m/s)*

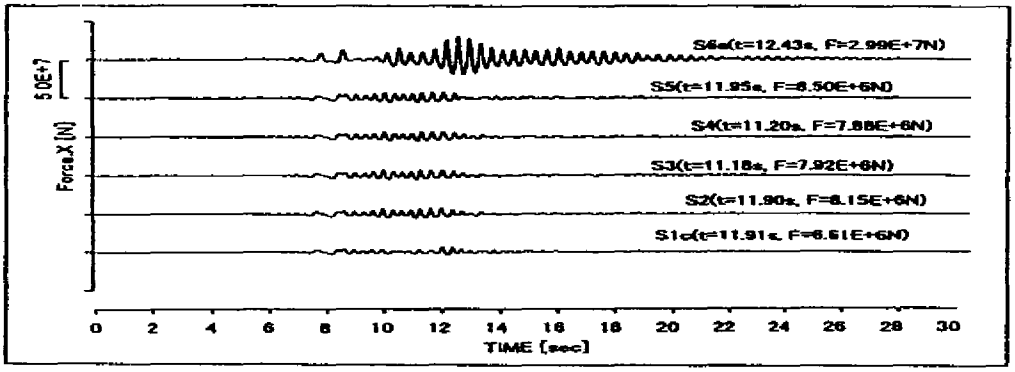


*Figure 17. Time-history of forces acting on fixed bearings (Model A-2, Va=3,000 m/s)*

**Effects of pounding between decks on collapse of bridges:**

Dynamic fracture analyses of the bridges were carried out by using apparent wave velocity, Va=3,000 (m/s). Figures 18 and 19 show the simulation results. Figure 19 is a close up of the dynamic displacement response during 7 to 10 (sec) in which severe poundings are observed. From these figures, we can say that due to a series of poundings between decks propagating from east to west, all the fixed bearings broke around 8 (sec) resulting two simply supported decks of the elevated bridge fell down as shown in Figure 20. The collapse mode obtained here is very similar to that of actual damage as shown in Photo 4. The difference between actual case and simulation is that S3 and S4 decks fell down in real damage, while S2 and S3 did in the simulation. Considering the uncertainties of input ground motions and some boundary conditions, this simulation results explains the mechanism of the damage as shown in Photo 4. As a next case, simulation using the Model A-2, in which S1 and S6 are divided, was carried out. Figure 21 shows the dynamic displacement response of each deck. Comparing the result with normal case as shown in Figure 18, it should be noted that the displacements are relatively very small and the effects of different dynamic properties of bridges played an important role in collapse mechanism.

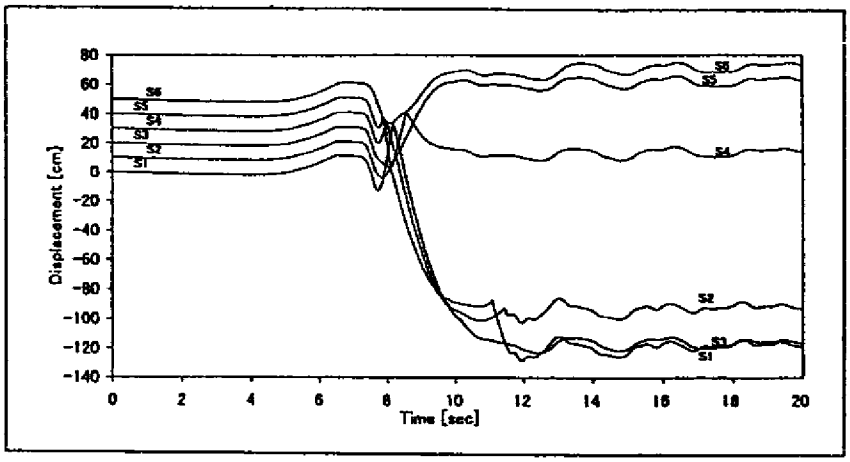


*Figure 18. Dynamic displacement response of each deck during collapse process (Model A-1, Va=3,000m/s)*

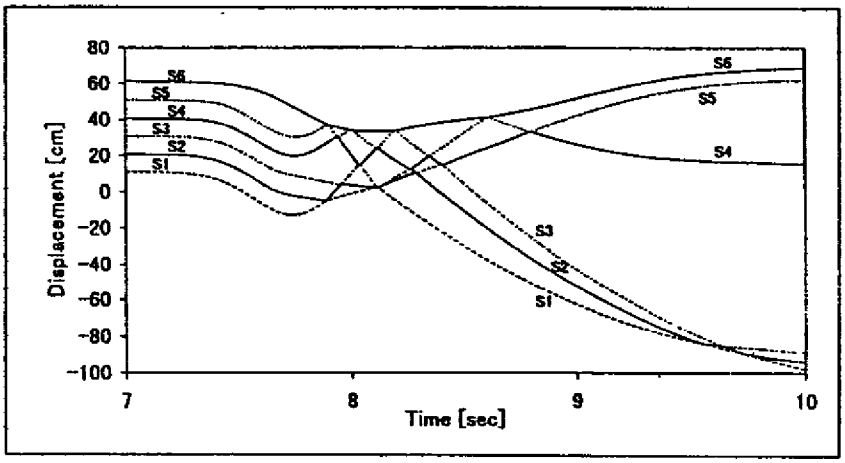


*Figure 19. Close up of the displacement response during 7 to 10 sec (Model A-1, Va=3,000m/s)*

### 3.2 Simulation Results using Model B

With the model in Figure 11, collapse process of the damage to elevated expressway bridges due to overturning was simulated. This was the symbolic damage during the Kobe earthquake shown in Photo 5. Simulations of collapse process of two different cases (B-1 and B-2) are shown in Figure 22. Figure 22 (a) is a result under condition that the pier has an uniform strength from the top to the bottom (B-1), while the pier in Figure 22 (b) has a discontinuous plane where the reinforcement ratio changes similar to the same as real case(B-2). Figure 23 shows the displacement-acceleration relation of the deck. With time, the bridge inclined and finally, overturned. Although the exact collapse process is not reported, the final collapse modes obtained in this study agree with those of the real damage.

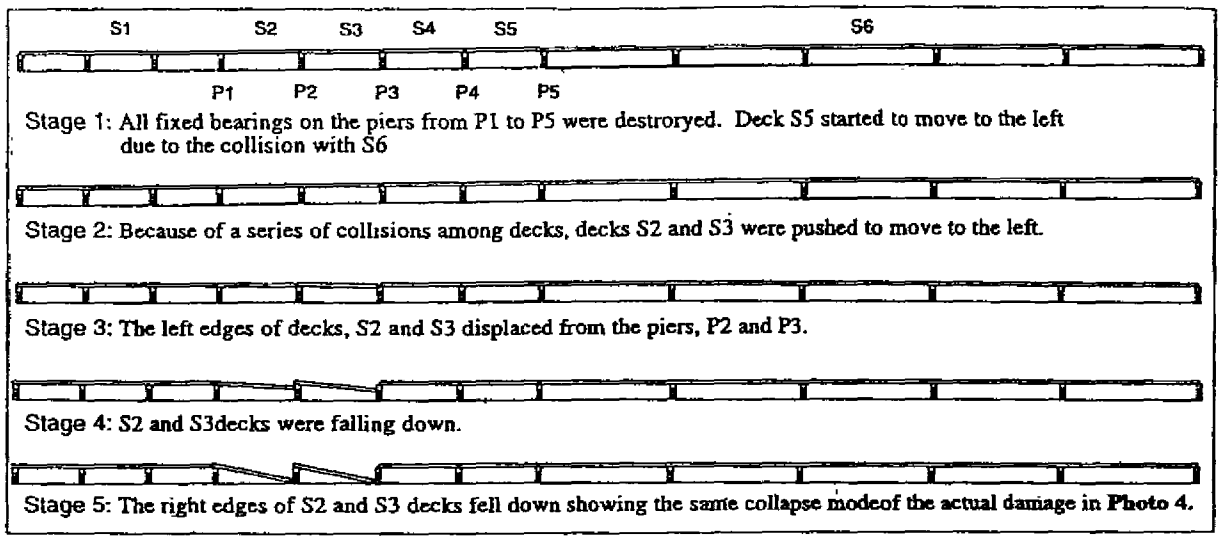


*Figure 20 (a). EDE Simulation of collapse process of elevated expressway bridges (Model A-1, Va=3,000 m/s)*

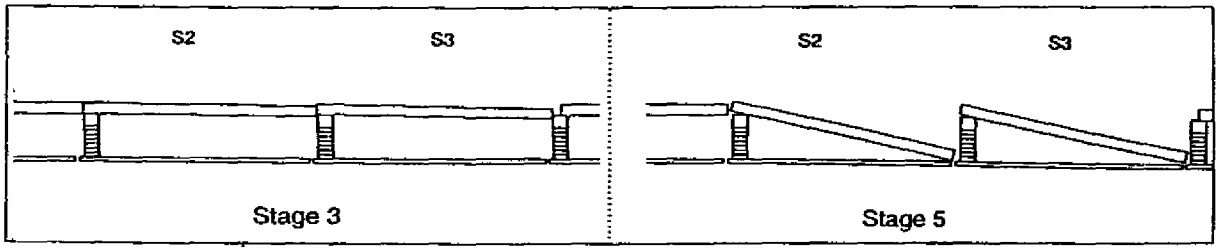


*Figure 20(b). Close up of collapsed parts*

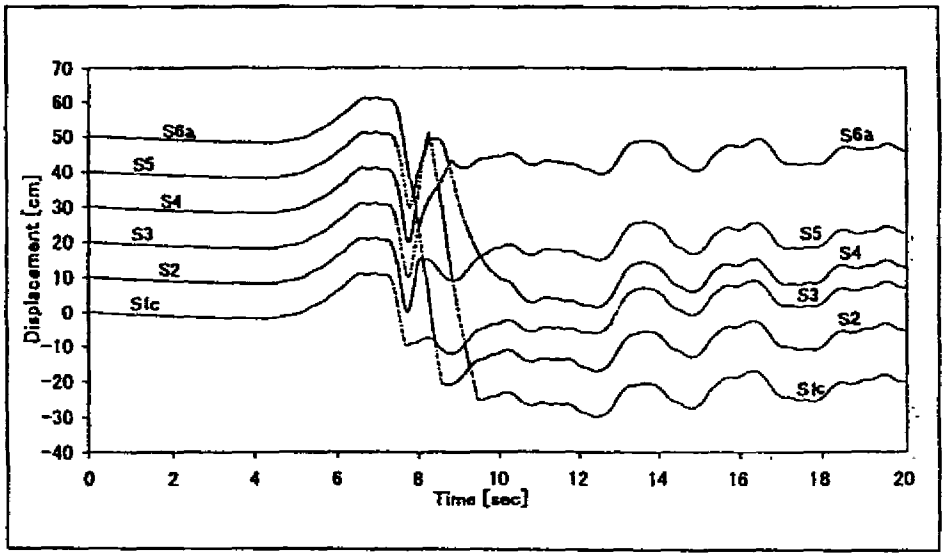


*Figure 21. Dynamic displacement response of each deck during collapse process (Model A-2, Va=3,000m/s)*

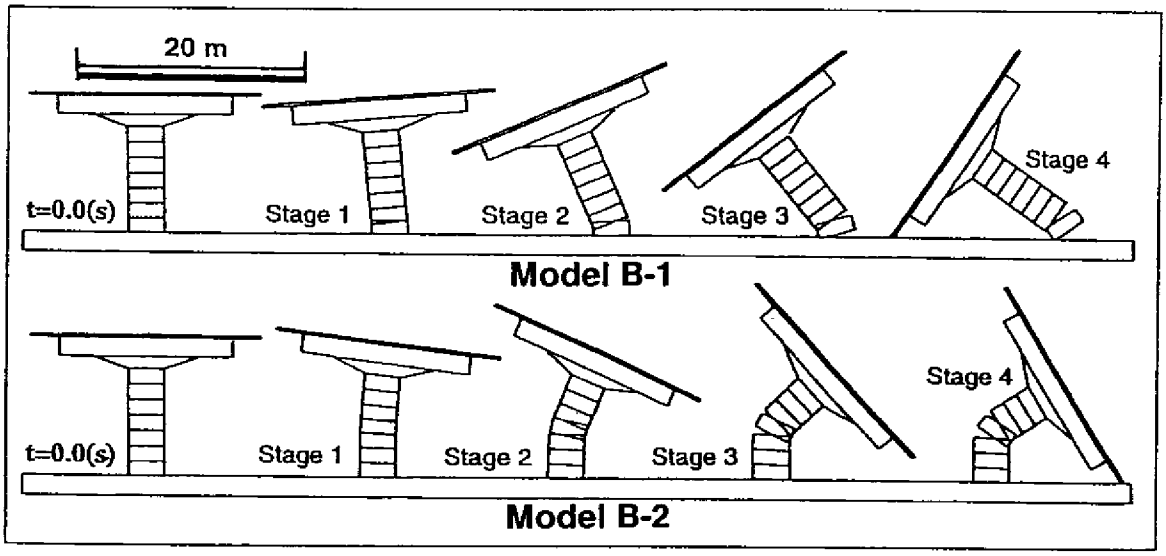


*Figure 22. EDE simulation of collapse process of pilz-type elevated expressway bridges (Model B)*

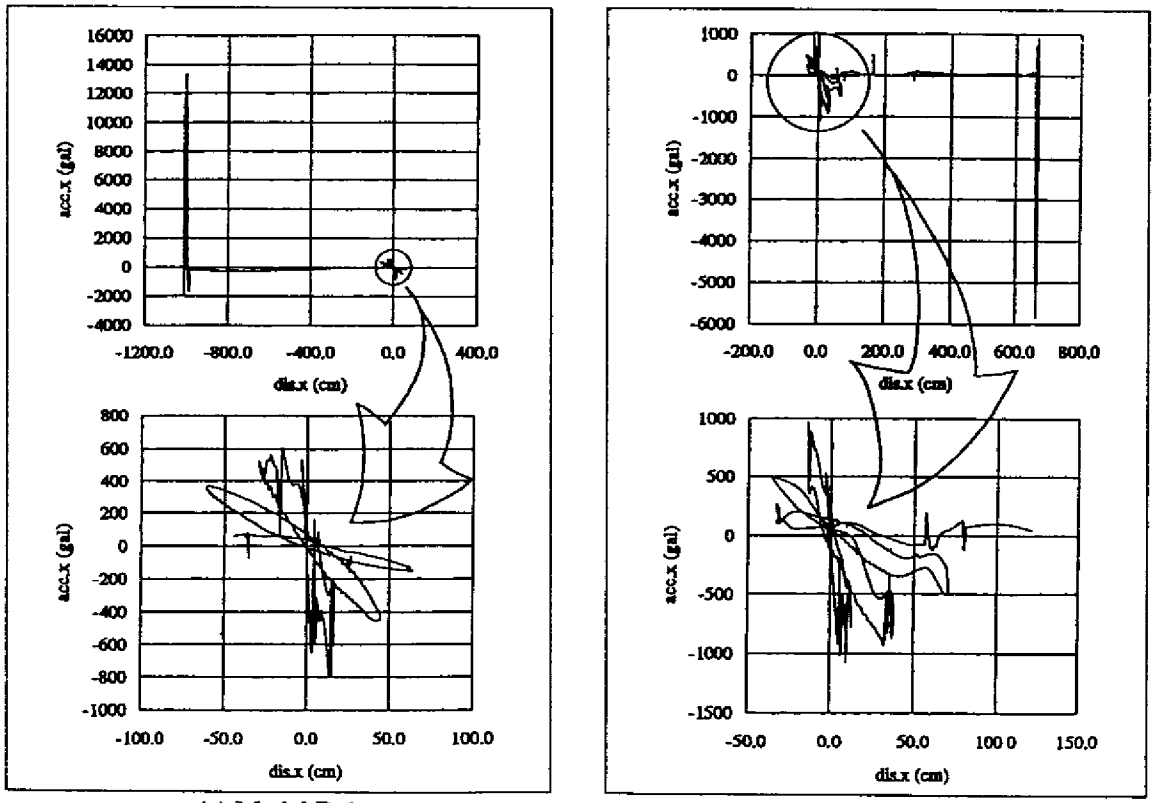


(a) Model B-1 (b) Model B-2

*Figure 23 Displacement-acceleration relation of the deck (Model B)*

## 4. CONCLUSION

Using the EDEM, we tried to simulate the collapse process of structures due to the Kobe earthquake in order to study the mechanism of the damage. These simulations are based on the new concept of the EDEM application in which the EDEM is taken as an enhanced lumped mass system. Although the phenomena treated in this study were difficult to be simulated by the conventional methods such as the finite element method, the numerical results obtained by the EDEM agree well with the real earthquake damage.

Examining the simulation results, a conclusion can be drawn that the macro models of these structures would be capable of demonstrating to some extent as to how structures would undergo local collapse, whereby the models be allowed to account for the process or the mechanism of actual earthquake-caused structural collapse with certain accuracy. Although the EDEM is required to go through improvements over various points, the results for fracture as a whole, generally replicate observed earthquake damage.

## REFERENCES


1. Cundall, P. A. (1971). "A computer model for simulating progressive, large scale movement in blocky rock Systems", *Proc. of Symp. ISRM*, Nancy, France, Vol 2, pp. 129-136.

2. Hakuno, M. and K. Meguro (1993). "Simulation of concrete-frame collapse due to dynamic loading", *ASCE Journal of Engineering Mechanics*, **119**, (9), pp. 1709-1723.

3. Iwashita, K. and M. Hakuno (1990). "Modified distinct element method simulation of dynamic cliff collapse", *Structural Eng./Earthquake Eng.*, Japan Society of Civil Engineers (JSCE), **7**, (1), pp. 133-142.

4. Meguro, K., K. Iwashita and M. Hakuno (1988) "Fracture tests of masonry concrete elements by granular assembly simulation", *Proc. of 9WCEE*, Vol. 6, pp. 181-186.

5. Meguro, K. and M. Hakuno (1989a). "Fracture analyses of concrete structures by the modified distinct element method", *Structural Eng./Earthquake Eng* , JSCE, **6**, (2), pp. 283-294.

6. Meguro, K. and M. Hakuno (1989b). "Extended distinct element analysis of collapse process of structures", *Proc. of 10th Annual Conf. on Natural Disasters*, Japan society on natural disaster science, pp. 26-27 (in Japanese)

7. Meguro, K., K. Iwashita and M. Hakuno (1991). "Fracture analyses of media composed of irregularly shaped regions by the extended distinct element method", *Structural Eng./Earthquake Eng* , JSCE, **8**, (3), pp. 131s-142s.

8. Meguro, K. and M. Hakuno (1992). "Simulation of collapse of structures due to earthquakes using the extended distinct element method", *Proc. of 10WCEE*, Vol. 7, pp. 3793-3796.

9. Meguro, K. and M. Hakuno (1994). "Application of the extended distinct element method for collapse simulation of a double-deck bridge", *Structural Eng /Earthquake Eng.*, JSCE, **10**, (4), pp. 175s-185s.